A triangular lattice model for binary and ternary mixtures containing surfactants

1994 J. Phys.: Condens. Matter 6 2799

(http://iopscience.iop.org/0953-8984/6/15/003)

J. Phys.: Condens. Matter 6 (1994) 2799–2812. Printed in the UK

A triangular lattice model for binary and ternary mixtures containing surfactants

Mohamed Laradji†, Hong Guo and Martin J Zuckermann

Centre for the Physics of Materials and Department of Physics, McGill University, Rutherford Building, 3600, Rue University, Montréal, Québec, Canada H3A 2T8

Received 11 October 1993, in final form 30 November 1993

Abstract. The phase equilibria of ternary mixtures of water, oil and surfactants and binary mixtures of water and surfactants are studied using a triangular lattice-gas model that is an extension of the spin-1 Blume–Capel model with the addition of the orientational degrees of freedom for surfactants. The phase diagram of the model is investigated via Monte Carlo simulations in conjunction with the extrapolation technique of Ferrenberg and Swendsen combined with the finite-size scaling method of Lee and Kosterlitz. Five phases are found for ternary mixtures in the case of equal water and oil concentrations: a water–oil coexistence region, a lamellar phase, a liquid crystalline phase, which has the symmetry of a rhombic lattice, and an extended disordered phase, which is divided by a Lifshitz line into disordered fluid and microemulsion regions. In the limiting case of a binary mixture of water and surfactants, we found a rich phase diagram corresponding to a lamellar phase, a hexagonal phase and a disordered phase, which is again divided by a Lifshitz line into disordered fluid and structured fluid regions. The latter can be considered as the analogue of the microemulsion found for the ternary systems.

1. Introduction

Mixtures containing surfactants have attracted considerable attention due to their potential for industrial applications [1]. These mixtures are complex fluids, which exhibit many distinct fluid phases having structures differing greatly from ordinary simple fluids. The main ingredient giving rise to these structured fluids is the chemical nature of the surfactants. A surfactant molecule possesses two distinct groups that have vastly different solubilities although they are attached chemically [1]. There are several types of surfactant, for example amphiphilic molecules, which have a hydrophilic head group preferring a water environment and a hydrophobic tail, which prefers an oil-like environment.

When mixed with water and oil, surfactants screen the repulsive two-body interaction between water and oil molecules and hence cause a considerable reduction of the water–oil interfacial tension. This reduction depends on the concentration of surfactants and the resulting interfacial tension between water and oil can become negligibly small. The effect of the surfactants on the phase behaviour, as found experimentally, is as follows for a mixture with comparable concentrations of water and oil. First, a two-phase coexistence region between water and oil is observed for sufficiently small surfactant concentrations. This is followed by a three-phase coexistence between water, oil and a microemulsion phase. The microemulsion is a disordered phase with some short-range order, composed of mesoscopic

† Present address: Center for Simulational Physics, The University of Georgia, Athens, GA 30602, USA.

0953-8984/94/152799+14$19.50

domains of water and oil, with sizes of a few hundred Ångströms. These domains are separated by surfactant monolayers and connected to form a bicontinuous structure [2]. As the surfactant concentration is further increased, the mixture passes completely into the microemulsion phase. An important property of the microemulsion is that its short-range order is manifested by a peak at non-zero wave vector in the small-angle neutron scattering intensities [2–4]. This implies that the interconnected domains are correlated within short distances. It is also found that as the surfactant concentration is increased, the position of the peak increases, implying a decrease in the size of the microdomains. For even higher surfactant concentrations, the surfactant monolayers become stiffer since the interfacial bending elasticity contribution to the free energy becomes important. This results in a creation of liquid crystal phases with long-range order such as the lamellar, cubic and hexagonal phases found experimentally [1].

It is interesting to note that microemulsions do not have the same structure for all water concentrations. It is often found that when the concentrations of water and oil are quite different, the microdomains are organized into a globular structure. Although they still have a well defined average length scale in this case, the microdomains are not correlated since a peak at $q = 0$ is usually observed in the scattering intensity [5].

When the concentration of oil is zero, we have the limiting case of a binary mixture of water and surfactants. This mixture also exhibits a rich phase behaviour, which, to some extent, is quite similar to that of the ternary mixture [6–8]. In this case, the hydrophobicity of the tails causes the surfactants to self-organize into structures such as micelles and bilayers where the hydrophilic heads are in contact with water, while the tails are in contact with each other. Liquid crystalline phases such as lamellar and hexagonal phases are also observed. The phase diagram obtained for non-ionic surfactants can be described as follows. A disordered phase occurs for sufficiently low surfactant concentrations. This is followed at low temperatures by a sequence of liquid crystal phases with long-range order. At higher temperatures, the disordered phase crosses over to a second disordered regime, in which surfactants are organized into an interconnected network of bilayers analogous to bicontinuous microemulsions. This disordered structure has a characteristic length scale, which again is manifested by a peak at a non-zero wave vector in the scattering intensity [7, 8].

Theoretical studies on these systems have made use of either lattice models or phenomenological Ginzburg–Landau models [9–12] in which the microscopic properties of the three components are coarse grained. The lattice models are on a molecular level since they mimic the interactions of individual surfactants with water and oil molecules respectively. Even though the models are constructed such that the water, oil and surfactant molecules have the same size, they have been quite successful in describing the main features of the phase diagram for these ternary mixtures [13–17]. The lattice models can be further grouped into two kinds. For the first kind, the surfactants are taken as isotropic molecules and their effect is described either by long-range interactions as in the Wheeler–Widom model [13, 14] or by a three-body interaction as in the Schick–Shih–Gompper model [16, 17]. The second kind of lattice model includes the intrinsic anisotropy of the surfactant molecules by assigning an orientation to each surfactant molecule [18–21]. These models have been studied in detail on square and cubic lattices [18–21] and Matsen *et al* recently studied a model of this type on an FCC lattice using the Bethe approximation [22]. The latter model takes into account the orientation of water molecules and includes hydrogen bonding between water and surfactants.

The purpose of this article is to report further theoretical studies of the phase behaviour of ternary and binary surfactant mixtures, using an appropriate lattice model that belongs to

the second kind mentioned above. We will restrict ourselves to two dimensions and study our model on a triangular lattice. This is an extension of our previous work on a square lattice, which was used to examine the phase diagram of the ternary mixture [20]. While the type of lattice basically affects non-universal properties of the system, we found that it is technically advantageous to use a triangular lattice, which has a larger coordination number and gives a better description of the curvature of the surfactant monolayers. This allows for a better description of the liquid crystal phases especially for the binary mixture.

The equilibrium phase diagrams for both the ternary and the binary systems were obtained from Metropolis Monte Carlo simulations in conjunction with the extrapolation technique due to Ferrenberg and Swendsen [23]. The order of the phase transitions was analysed via the finite-size scaling (FSS) method of Lee and Kosterlitz [24]. Five phases are found in ternary mixtures corresponding to water and oil-rich phases: a lamellar phase, which consists of alternating layers of water and oil separated by surfactant monolayers; a second liquid crystalline phase with rhombic symmetry and a disordered phase, which can be identified as a microemulsion beyond a Lifshitz line for a wide range of temperatures and surfactant concentrations. In agreement with experiment, we found that the position of the peak in the microemulsion structure factor increases with increasing surfactant concentration. Binary mixtures composed of water and surfactants were found to exhibit fewer phases: a lamellar phase composed of surfactant bilayers separated by water layers, a hexagonal phase and a disordered phase. The disordered phase has a similar structural behaviour to that found for the ternary case since it is again divided by a Lifshitz line into an ordinary fluid region and a structured fluid region. The latter has a well defined characteristic wavelength defined by a peak at non-zero wave vector in the structure factor and its position increases with increasing surfactant concentration.

This paper is organized as follows. The model and the numerical method are presented in sections 2 and 3, and the calculated phase diagrams of the model are given in section 4 for both the ternary and binary systems. A discussion of our results and a summary are given in section 5.

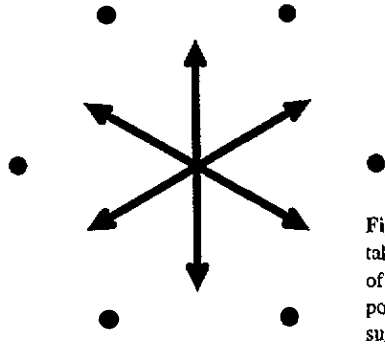

Figure 1. The six possible orientations that may be taken by a surfactant molecule. Note that instead of pointing towards a neighbouring site, a surfactant points between two neighbouring sites. In this way, a surfactant may interact with four water or oil molecules.

2. Model

In the present model [18–21], the oil, water and surfactant molecules each occupy a single site on a triangular lattice. This is included in the formalism by defining a spin-1 variable, σ_i, which takes values of $+1$, -1 or 0 for a water molecule, an oil molecule or a surfactant

molecule respectively at each site. In addition, a vector, m_i, is assigned to every surfactant molecule in order to describe the orientational degrees of freedom. In this way, we can write the Hamiltonian in terms of short-range two-body interactions. The six possible orientations of a surfactant molecule are displayed in figure 1 for the triangular lattice. The Hamiltonian is written as follows:

$$\mathcal{H} = -\sum_{\langle i,j \rangle} \left[J_1 \sigma_i \sigma_j + \frac{2}{\sqrt{3}} J_2 (\sigma_j \boldsymbol{m}_i \cdot \boldsymbol{r}_{ij} + \sigma_i \boldsymbol{m}_j \cdot \boldsymbol{r}_{ji}) \right] - \mu_s N_s - \mu_w N_w - \mu_o N_o \tag{1}$$

where $\langle i, j \rangle$ implies that the sum is over nearest neighbours. Here the first term in the sum corresponds to the spin-1 Blume–Capel model [26]. The second term in the sum is essential for surfactants since it represents two-body interactions between a surfactant and a water or an oil molecule. These interactions represent surfactant action at an oil–water interface, i.e., the head of a surfactant molecule prefers to orient towards a water-rich environment, whereas its tail prefers to orient towards an oil-rich environment. In particular, the surfactants are oriented parallel to the directions of the bisectors of neighbouring lattice bonds. Furthermore, a surfactant is allowed to interact simultaneously with four of its six nearest neighbours and preferentially with two water and two oil molecules (see figure 1). $\boldsymbol{r}_{ij}$ in equation (1) is a unit vector pointing from a site i towards a nearest-neighbour site j. $\boldsymbol{m}_i$ is a vector that is zero when i is occupied by either a water or an oil molecule, but becomes a unit vector when i is occupied by a surfactant. The last three terms in equation (1) give the chemical potentials of the three components. Noting that $N_s = \sum_i (1 - \sigma_i^2)$ and that $N_w - N_o = \sum_i \sigma_i$ and defining

$$\Delta = \mu_s - \tfrac{1}{2}(\mu_w + \mu_o) \tag{2}$$

the Hamiltonian in equation (1) can be written as follows:

$$\mathcal{H} = -\sum_{\langle i,j \rangle} \left[J_1 \sigma_i \sigma_j + \frac{2}{\sqrt{3}} J_2 (\sigma_j \boldsymbol{m}_i \cdot \boldsymbol{r}_{ij} + \sigma_i \boldsymbol{m}_j \cdot \boldsymbol{r}_{ji}) \right] + \Delta \sum_i \sigma_i^2 - \frac{1}{2}(\mu_w - \mu_o) \sum_i \sigma_i. \tag{3}$$

This model is relatively uncomplicated since it contains only one free parameter: J_2/J_1.

As stated above, we concentrate on the case of the three-component system where the concentrations of water and oil are equal (i.e., $\mu_w = \mu_o$), and the case of the two-component system of water and surfactants where the values of σ_i are restricted to $+1$ and 0.

3. Numerical methods

At finite temperatures we performed Metropolis Monte Carlo simulations in conjunction with the Ferrenberg–Swendsen extrapolation method [23]. In this method, it is sufficient to know the probability distribution at a temperature T and a chemical potential Δ in order to find the probability distribution at any other temperature T' and chemical potential Δ'. This allows one to calculate averaged quantities such as the internal energy, the surfactant density, the difference between the density of water and that of oil and their respective fluctuations at (T', Δ') from a knowledge of the distribution at (T, Δ). We can now numerically calculate the histogram proportional to the probability distribution. In order to generate a large

number of configurations efficiently so as to obtain accurate statistics, one expects that the extrapolations can be performed most efficiently close to phase transitions [23].

FSS analysis must be performed to determine the order of a phase transition. Usually one applies FSS to thermodynamic functions such as the heat capacity or susceptibility. It may, however, be difficult to ascertain the nature of the phase transition using these quantities since their FSS behaviour may be observable only for large system sizes. We therefore used a new numerical technique developed by Lee and Kosterlitz, which is able to establish the nature of phase transitions from the behaviour of small systems [24]. This method consists of calculating the free energy from the probability distribution. It has been shown [24] that for a first-order phase transition this free energy has the shape of a double well where the two minima occur at the energies (or the densities or the magnetizations) of the two coexisting phases. In this case, the height of the double well increases with increasing system size. For a second-order phase transition the free energy again has the shape of a double well for small system sizes. In this case, however, the double-well height remains unchanged as the system size increases. In the absence of a phase transition, the double well, if it occurs at small system sizes, will decrease and eventually vanish as the system size increases.

4. Calculated phase diagrams

4.1. The $T = 0$ phase diagram

The phase diagram at $T = 0$ can be determined exactly. Five phases were found for equal concentrations of water and oil. They correspond to the pure water and oil phases, a lamellar phase, which corresponds to monolayers of surfactants separating water and oil layers, a liquid crystal phase, which has the symmetry of the rhombic lattice with its structure shown in figure 2(a), and finally a pure surfactant phase. Since surfactant–surfactant interactions are omitted in the Hamiltonian of (3), the surfactants are randomly oriented in the surfactant phase. This is not in agreement with the experimental situation, where surfactants are organized into structures with long-range order. Consequently, for this model, the surfactant phase is the extension of the disordered phase to $T = 0$. The phase diagram of the model at $T = 0$ in the ternary case is shown as a function of J_2/J_1 and Δ/J_1 in figure 3(a).

The ground states of the binary mixture of water and surfactants are determined in the same way. In this case three phases are found. They correspond to a lamellar phase, which can be described in terms of bilayers of surfactants separating monolayers of water, a hexagonal phase corresponding to sites occupied by water on a triangular sublattice and surrounded by surfactants as shown in figure 2(b), and finally the same pure surfactant phase as found for the three-component case. The phase diagram of the two-component mixture is shown as a function of J_2/J_1 and Δ/J_1 in figure 3(b). From these two phase diagrams, we conclude that the liquid crystalline phases are only observed for relatively strong surfactants, i.e., for $J_2/J_1 > \frac{1}{2}$.

We have chosen to study the model with $J_2/J_1 = 2$ and do not expect any significant change in the global phase behaviour of the model as long as $J_2/J_1 > \frac{1}{2}$, since the sequences of phases of figure 3(a) and 3(b) is the same for this range of surfactant interactions.

4.2. The ternary mixture

We next show results for the phase diagram of the ternary mixture of water, oil and surfactants when the average concentrations of water and oil are equal.

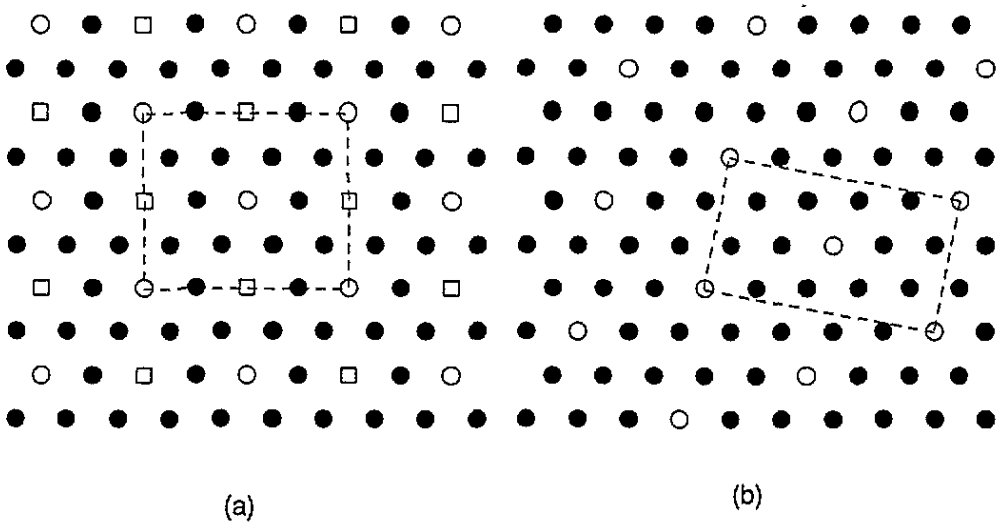

Figure 2. Ground state configurations of the rhombic liquid crystal phase in the ternary case (a), and the hexagonal phase in the binary case (b). The dashed rectangles define the unit cell. The closed circles represent surfactant molecules, the open circles represent water molecules and the squares represent oil molecules.

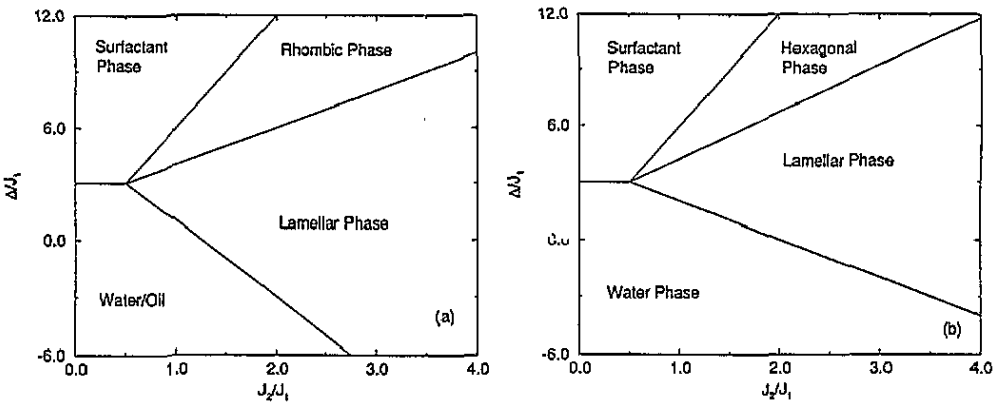

Figure 3. Ground state phase diagrams of the model, equation (3). (a) corresponds to the ternary case with $\mu_w = \mu_o$, and (b) corresponds to the binary case.

An approximate determination of the transition lines in the phase diagram was obtained from standard Monte Carlo simulations for several values of the chemical potentials, ranging from $\Delta = -14J_1$ up to $\Delta = 12J_1$, and several temperatures. The simulations were run for 4×10^6 Monte Carlo steps per site on various system sizes.

The phase diagram of the model is shown in figure 4 as a function of reduced temperature k_BT/J_1 and reduced chemical potential Δ/J_1. As pointed out above, five phases are observed. A broad water–oil coexistence region is found, which extends to large negative values of Δ/J_1. The concentration of surfactants is very low in this region. The transition line separating the region of water–oil coexistence from the disordered phase is mostly second order. We note that when Δ becomes very large and negative such that there are

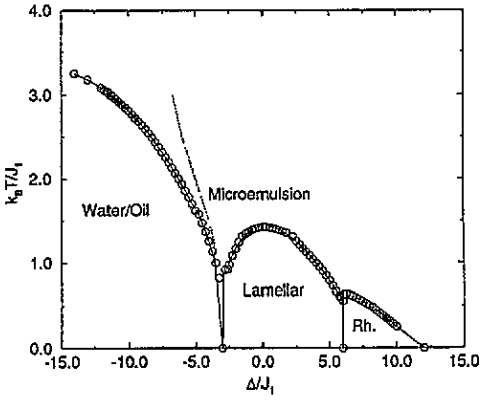

Figure 4. Monte Carlo phase diagram of the ternary mixture of water, oil and surfactants with $\mu_w = \mu_o$ and $J_2 = 2J_1$.

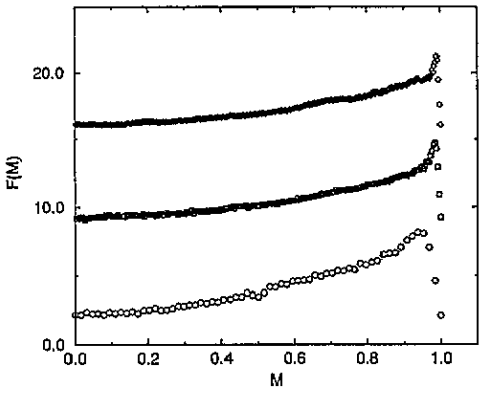

Figure 5. Free energy as a function of $M = \sum_i \sigma_i / L^d$ with $\Delta = -3.5J_1$ for $L = 8$ (circles), $L = 16$ (squares) and $L = 20$ (diamonds).

essentially no surfactants in the system, the model is a spin-1 Ising model. Indeed in this limit, the transition line approaches the critical temperature of the triangular lattice Ising model $k_B T_c = 3.641 J_1$ [27].

At chemical potentials larger than $\Delta \simeq -4J_1$, triple-well structure is detected in the free energy versus $M = \sum_i \sigma_i / L^d$ as shown in figure 5. The three minima occur at $M = 0$ corresponding to the disordered phase and at $M = \pm 1$ corresponding to the water and oil phases. As the system size increases, the double-well structure becomes sharper leading to an uncertainty in the height of the free energy barrier. The presence of such a well is an indication that the phase transition from the water–oil coexistence region to the disordered phase is first order. Indeed, the 129^2 configuration shown in figure 6, which was obtained at $\Delta = -3.5J_1$ with fixed boundary conditions along one direction and periodic boundary conditions along the other direction, clearly shows a three-phase coexistence of the water, the oil and the disordered phases. The initial configuration for this case was a 128×30 strip of water plus a strip of oil of the same dimensions. Each strip was adjacent to the appropriate fixed boundaries and the remaining sites were chosen as a completely disordered mixture of all three components. The snapshot shown in figure 6 represents the configuration found after 10^5 MCS per site. The presence of a triple line of coexistence and a line of second-order transitions implies the presence of a tricritical point. We were, however, not able to determine its exact location.

A lamellar phase is observed at low temperatures for chemical potentials larger than $\Delta = -3J_1$. The FSS analysis of the phase transition from the lamellar phase to the disordered phase shows that this phase transition is always first order. It is interesting to note that there is no three-phase coexistence between the lamellar, the water and the oil phases except at $T = 0$. This allows the disordered phase to extend to zero temperature between the water–oil coexistence curve and the lamellar phase as was previously observed in several models [17, 20, 28, 12].

At higher surfactant chemical potentials, the system undergoes a transition from the lamellar phase to a liquid crystal phase with rhombic symmetry (see figure 2(b)). Again from an FSS analysis of the free energy barrier, we found that this phase transition is first order.

It is worth noting that mean field calculations of the phase transition lines from the

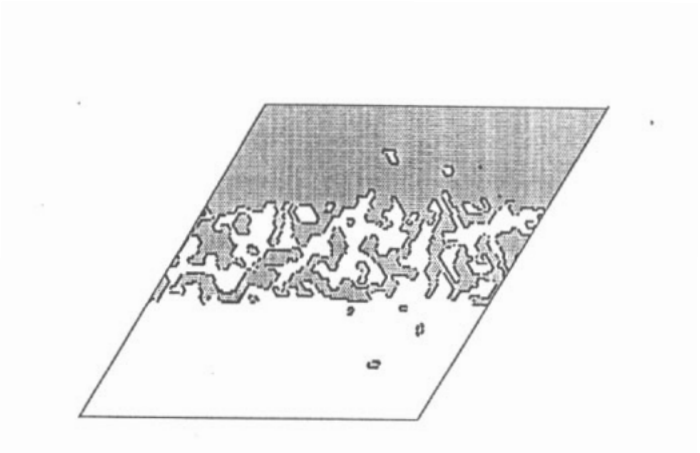

Figure 6. A configuration in a three-phase coexistence between the water, the oil and the disordered phases at $\Delta = -3.5J_1$ and $k_BT = 101J_1$. The system size is 129×129.

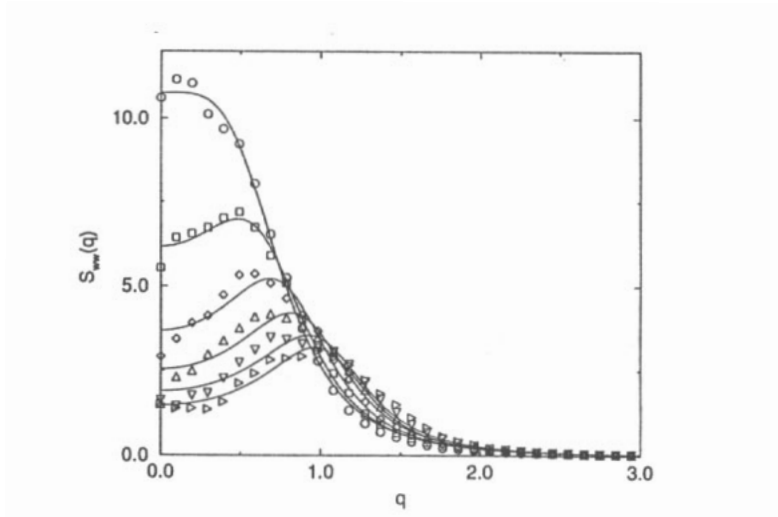

Figure 7. The structure factor in the microemulsion regime of the disordered phase at $k_BT = J_1$ and $\Delta = -3.4J_1$ (○), $\Delta = -3.2J_1$ (□), $\Delta = -3J_1$ (◇), $\Delta = -2.8J_1$ (△), $\Delta = -2.6J_1$ (▽) and $\Delta = -2.4J_1$ (▷). The solid lines are guides for the eye.

lamellar phase to the rhombic phase and from the rhombic phase to the disordered phase can easily be performed at low temperatures, and their respective equations are given by

$$\frac{\Delta}{J_1} = \frac{2J_2}{J_1} + 2 - \frac{k_BT}{J_1}\ln 2 \tag{4}$$

and

$$\frac{\Delta}{J_1} = \frac{6J_2}{J_1} + \frac{k_BT}{J_1}(\ln 2 - 4\ln 6). \tag{5}$$

The low-temperature mean field phase boundaries are in good agreement with the Monte Carlo results of figure 4.

Figure 4 shows that the disordered phase can be divided into two sub-regions with different short-range structures by a Lifshitz line. The Lifshitz line is not a phase boundary

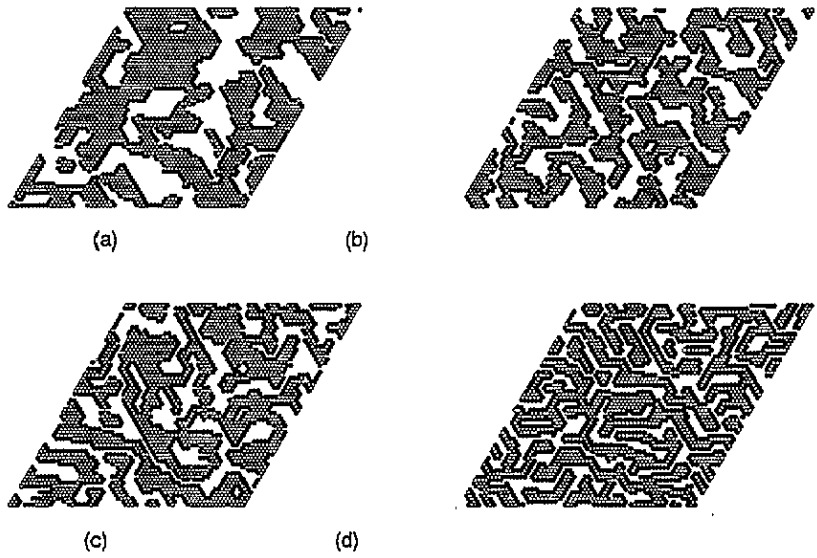

Figure 8. Configurations in the disordered phase at $k_BT = J_1$. (a), (b), (c) and (d) correspond respectively to $\Delta = -3.4J_1$, $-3.2J_1$, $-3.0J_1$ and $-2.4J_1$.

since no singularities are encountered in the derivatives of the free energy. To the left of the Lifshitz line, the structure factor of the disordered phase peaks at $q = 0$. Systems in this sub-region can therefore be identified as simple fluids. To the right of the Lifshitz line, the structure factor of the disordered phase exhibits a peak at a non-zero value, q_{max}. In figure 7, we show the structure factor as a function of surfactant concentration in the narrow region between the water–oil coexistence and the lamellar phase at $k_BT/J_1 = 1$ [29]. We observe that as the surfactant concentration is increased, q_{max} increases, implying a decrease in the size of the microdomains as displayed by the real-space configurations in figure 8. In these configurations, we observe that most of the surfactants are adsorbed at the water–oil interfaces. At higher temperatures the solubility in water and oil becomes higher, as expected.

4.3. The binary mixture

We next study the limiting case where the concentration of oil is zero. The phase diagram for such binary fluid mixtures was determined in the same manner as for the case of the ternary mixture discussed above. As before, the simulations were run for 4×10^6 MCS per site on several system sizes.

The phase diagram of the binary mixture is shown in figure 9. Only three phases are observed in this case. For $\Delta/J_1 < 0$ a pure water regime is observed at low temperatures. This regime crosses to a disordered regime with non-zero surfactant concentration at the dotted line shown in figure 9. It is important to note that this line does not correspond to a phase boundary, since although a peak in the heat capacity is observed at this line, the value of the maximum of the heat capacity does not increase with increasing system size. Mean field calculations for this model also predict a finite peak in the heat capacity in this region of the phase diagram. In fact, in this case the model reduces to the spin-$\frac{1}{2}$ Ising model in a magnetic field, which does not exhibit a phase transition. This implies that the disordered phase extends to zero temperatures for chemical potentials smaller than $\Delta/J_1 = 0$.

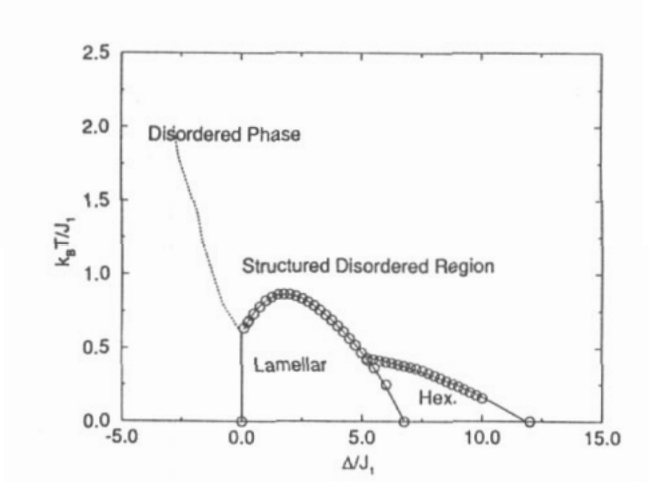

Figure 9. The Monte Carlo phase diagram of the binary mixture of water and surfactants with $J_2 = 2J_1$.

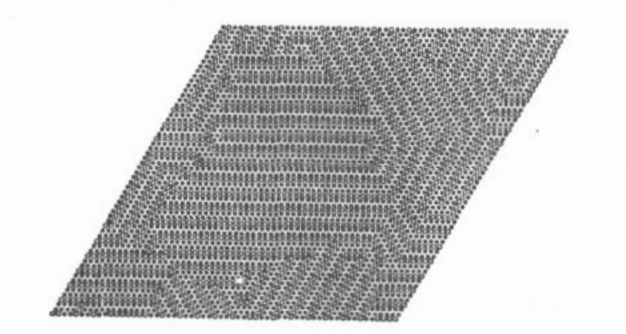

Figure 10. A lamellar configuration in the lamellar phase of figure 9. Open circles represent water molecules and closed circles represent surfactants.

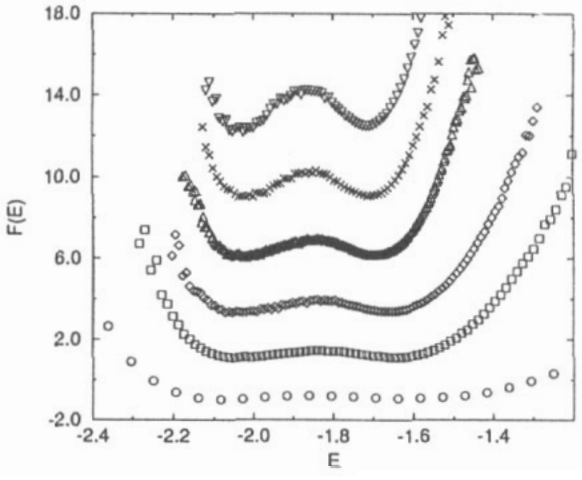

Figure 11. The free energy as a function of internal energy at $\Delta = 2J_1$ for the following system sizes: $L = 6$ (○), $L = 9$ (□), $L = 15$ (◇), $L = 24$ (△), $L = 30$ (×) and $L = 36$ (▽).

The water-rich region is followed by a lamellar phase for which a sample configuration is displayed in figure 10. The transition separating the lamellar phase from the disordered phase is found to be first order by FSS analysis. The free energy was obtained as a function

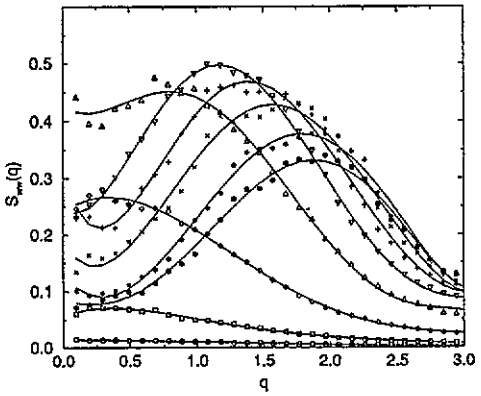

Figure 12. The water–water structure factor in the disordered regime of figure 9 at $k_BT = J_1$ for the following surfactant chemical potentials: $\Delta = -2J_1$ (○), $\Delta = -1.6J_1$ (□), $\Delta = -1.2J_1$ (◇), $\Delta = -0.8J_1$ (△), $\Delta = -0.4J_1$ (▽), $\Delta = 0$ (+), $\Delta = 0.4J_1$ (×), $\Delta = 1.2J_1$ (*), and $\Delta = 2J_1$ (●). The solid lines are guides for the eye.

of surfactant concentration and is displayed for several systems sizes in figure 11 when $\Delta/J_1 = 2$. This figure clearly shows that the height of the double well increases as the system size increases. Thus the transition from the lamellar phase to the disordered phase is first order. As the surfactant chemical potential is further increased, the lamellar phase crosses to a second liquid crystal phase with a hexagonal symmetry whose microstructure is shown in figure 2(b). The nature of the phase transition from this phase to the lamellar and disordered phases is also first order.

As in the case of ternary mixtures, we calculated the transition lines between the various phases using mean field theory. The equation of the low-temperature transition line from the water-rich region of the disordered phase to the lamellar phase is given by

$$\frac{\Delta}{J_1} = 4 - 2\frac{J_2}{J_1} \tag{6}$$

and is independent of temperature. The equation of the phase boundary from the lamellar phase to the hexagonal phase is given at low T by

$$\frac{\Delta}{J_1} = \frac{5J_2}{2J_1} + \frac{7}{4} - \frac{9k_BT}{2J_1}\ln 2. \tag{7}$$

Finally the equation of the phase boundary between the hexagonal phase and the disordered phase at low T is

$$\frac{\Delta}{J_1} = \frac{6J_2}{J_1} + \frac{k_BT}{J_1}(6\ln 2 - 7\ln 6). \tag{8}$$

All three results are in agreement with the Monte Carlo phase diagram of figure 9.

The disordered phase in the phase diagram of figure 9 can also be divided into two sub-regions by a Lifshitz line. To the left of the Lifshitz line the structure factor of the disordered phase has a peak at $q = 0$. Again, to the right of the Lifshitz line, the structure factor of the disordered phase exhibits a well defined broad peak whose position increases as the surfactant concentration is increased, as shown in figure 12. The region to the right of

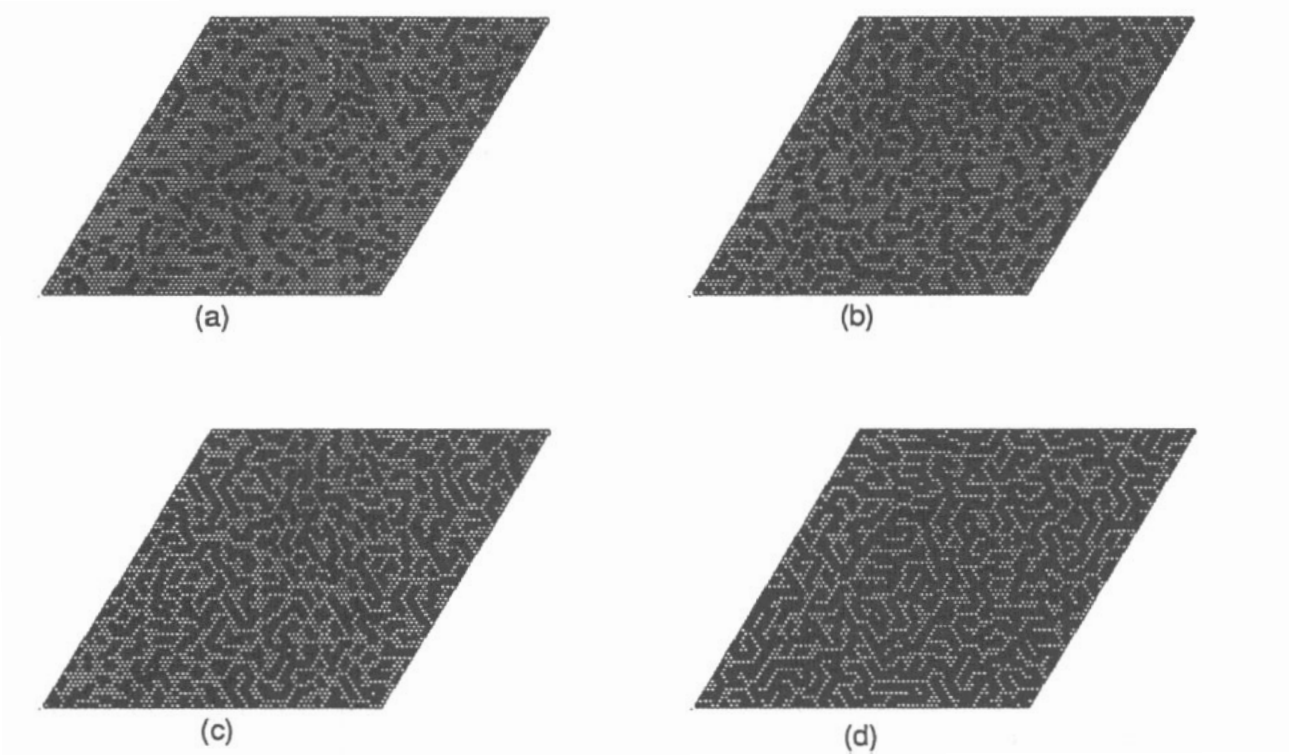

Figure 13. Monte Carlo configurations in the disordered phase at $k_B T = J_1$. (a), (b), (c) and (d) correspond respectively to $\Delta = -0.4J_1$, $\Delta = 0$, $\Delta = 0.4J_1$ and $\Delta = 1.2J_1$. Open circles represent water molecules and closed circles represent surfactants.

the Lifshitz line of the phase diagram is a structured fluid region, which can be considered as the analogue of the bicontinuous microemulsion in the ternary case. This behaviour has been observed in experiments [7] and in previous mean field calculations [30]. As was the case for the bicontinuous microemulsions the presence of this peak implies that the water domains (or the surfactant bilayers) are correlated. Indeed, the real-space configurations corresponding to these structure factors are shown in figure 13, where we find a network of surfactant bilayers that exhibit short-range order. This can be seen clearly in figure 13(d), which shows many water lines along lattice directions. This occurs because the structured fluid region is the disordered region to which the lamellar phase makes a transition as the temperature is increased. The lines of water and the neighbouring surfactants then represent residual lamellar fragments in this disordered region. The water lines are no longer observed for sufficiently high values of the chemical potential.

5. Discussion

In this paper we present a triangular lattice model for surfactants in binary and ternary mixtures. The phase diagram of the model was calculated in detail for ternary mixtures of water, oil and surfactants with equal average concentrations of water and oil, and for binary mixtures of water and surfactants. In both cases, the transition lines were determined via the extrapolation method of Ferrenberg and Swendsen combined with the FSS analysis of Lee and Kosterlitz. We found that the model exhibits a rich phase behaviour in qualitative agreement with experimental observations.

The following phases were found for the ternary case: a water–oil coexistence region, a lamellar phase, a liquid crystalline phase, which has the symmetry of a rhombic lattice, and a broad disordered phase divided by a Lifshitz line into an ordinary simple fluid region and a microemulsion region. The microemulsion in this region is the analogue of the bicontinuous microemulsion found in three-dimensional ternary mixtures containing surfactants for comparable water and oil concentrations. These are the same as what was found previously [20].

For the case of a binary mixture of water and surfactants, we found three phases. They correspond to a lamellar phase consisting of bilayers of surfactants separated by monolayers of water, a hexagonal phase with water organized into a hexagonal sublattice and coated by surfactant monolayers and a disordered phase. The latter phase is observed for very low or very high surfactant concentration and for high temperatures. The structure of the hexagonal phase allows us to identify it as the two-dimensional analogy of the inverted hexagonal phase observed experimentally [6, 7]. The disordered phase is divided into a simple fluid region for small concentrations of surfactants and a structured fluid region for high surfactant cocentrations. The latter is the analogue of the microemulsion region in the ternary mixture since it is characterized by a broad peak with its position increasing as the surfactant concentration increases. Furthermore, the position of the peak is higher than that of the microemulsion found for the ternary mixture. It is important to note that this phase diagram is qualitatively similar to that observed in experiments for non-ionic surfactants [6, 7]. It is therefore tempting to suppose that part of the disordered structured fluid region found in our simulations for the binary mixture containing surfactants is the two-dimensional analogue of a sponge phase [31]. However it is difficult to make an unambiguous identification.

We should mention that there are some limitations of the present model. Since hydrogen bonding between water molecules and surfactants is not included in this work, the two-phase coexistence between the disordered and water-rich phases seen experimentally in binary mixtures is not found from the present model. Also no hexagonal phase was found to the left of the lamellar phase in the phase diagram of figure 9. Such a phase is usually observed experimentally.

Since the model produces phase behaviour in qualitative agreement with the experimental observations, we are confident that it captures the essential physics of fluid mixtures containing surfactants. A three-dimensional version of this model is at present under investigation by Matsen *et al* [32]. An extension of this model to include the effects of hydrogen bonding between surfactant polar heads and water molecules, as suggested by Matsen *et al* [22], is also being studied.

Acknowledgments

The authors wish to thank Michael Schick for drawing their attention to the sponge phase and to John Ipsen, Don Sullivan and Michael Schick for stimulating discussions and helpful comments. This work is supported by the Natural Sciences and Engineering Research Council of Canada and Le Fonds pour la Formation des Chercheurs et l'Aide à la Recherche de la Province de Québec via both a Centre and a team grant.

References

[1] Meunier J, Langevin D and Boccara N (ed) 1987 *Physics of Amphiphilic Layers* part VI (Berlin: Springer) and references therein

[2] Auvray L, Cotton J P, Ober R and Taupin C 1984 *J. Physique* **45** 913; 1986 *Physica* B **136** 281
[3] Kotlarchyk M, Chen S-H, Huang J H and Kim M W 1984 *Phys. Rev. Lett.* **53** 941
[4] Alba-Simionesco C, Teixeira J and Angell C A 1989 *J. Chem. Phys.* **91** 395
[5] Kaler E W, Benett K E, Davis H T and Scriven L E 1984 *J. Chem. Phys.* **79** 5673
[6] Lang J C and Morgan R D 1980 *J. Chem. Phys.* **73** 5849
[7] Degiorgio V, Corti M and Cantú L 1988 *Chem. Phys. Lett.* **151** 349
[8] Strey R, Winkler J and Magid L 1991 *J. Phys. Chem.* 95 7502
[9] Safran S A and Turkevick L A 1983 *Phys. Rev. Lett.* **50** 1930
[10] Cates M E, Roux D, Andelman D, Milner S T and Safran S A 1988 *Europhys. Lett.* **5** 733
[11] Chen K, Jayaprakash C, Pandit R and Wenzel W 1990 *Phys. Rev. Lett.* **65** 2736
[12] Laradji M, Guo H, Grant M and Zuckermann M J unpublished
[13] Wheeler J and Widom B 1968 *J. Am. Chem. Soc.* **90** 3064
[14] Widom B 1986 *J. Chem. Phys.* **84** 6943
[15] Chen K, Jayaprakash C and Pandit R 1988 *Phys. Rev.* A **38** 6240
[16] Schick M and Shih W 1984 *Phys. Rev.* A **34** 1797
[17] Gompper G and Schick M 1989 *Phys. Rev. Lett.* **62** 1647; 1990 *Phys. Rev.* B **41** 9148; 1990 *Phys. Rev.* A **42** 2137
[18] Ciah A, Hoye J and Stell G 1989 *J. Chem. Phys.* **90** 1215
Ciah A and Hoye J 1989 *J. Chem. Phys.* **90** 1222
[19] Matsen M and Sullivan D E 1990 *Phys. Rev.* A **41** 2021; 1992 *J. Physique* II **2** 93
[20] Laradji M, Guo H, Grant M and Zuckermann M J 1991 *Phys. Rev.* A **44** 8184
[21] Laradji M 1993 *PhD Thesis* McGill University, Montreal, Canada
Slotte P A 1992 *Phys. Rev.* A **46** 6469
[22] Matsen M, Schick M and Sullivan D E 1992 *J. Chem. Phys.* **98** 2341
[23] Ferrenberg A M and Swendsen R H 1988 *Phys. Rev. Lett.* **63** 1195
[24] Lee J and Kosterlitz J M 1990 *Phys. Rev. Lett.* **65** 137
[25] Blume M 1966 *Phys. Rev.* **141** 517
Capel H W 1966 *Physica* **32** 966
[26] Baxter R J 1982 *Exactly Solved Models in Statistical Mechanics* (New York: Academic) pp 276–321
[27] Levin Y, Mundy C and Dawson K 1992 *Phys. Rev.* A **45** 7309
[28] The structure factors in both the ternary and binary cases are calculated on systems with a linear size $L = 64$
[29] Gompper G and Schick M 1989 *Chem. Phys. Lett.* **163** 475
[30] Cates M E 1991 *The Structure and Conformation of Amphiphilic Membranes* ed R Lipowsky, D Richter and K Kremer (Berlin:Springer) pp 275–80
[31] Matsen M, Sullivan D E and Zuckermann M J in preparation